Received: 28 October 2019 | Revised: 5 April 2020 | Accepted: 23 June 2020

DOI: 10.1002/hbm.25125

WILEY

RESEARCH ARTICLE

Loss of frontal regulator of vigilance during sleep inertia: A simultaneous EEG-fMRI study

Xinyuan Chen[1,2] | Ching-Fen Hsu[3] | Dan Xu[1,2] | Jing Yu[1,2] | Xu Lei[1,2]

[1]Sleep and NeuroImaging Center, Faculty of Psychology, Southwest University, Chongqing, China

[2]Key Laboratory of Cognition and Personality, Ministry of Education, Chongqing, China

[3]Research Center for Language Pathology and Developmental Neurosciences, College of Foreign Languages, Hunan University, Changsha, China

Correspondence
Xu Lei, Sleep and NeuroImaging Center, Faculty of Psychology, Southwest University, Chongqing 400715, China.
Email: xlei@swu.edu.cn

Funding information
Major Project of Medicine Science and Technology of PLA, Grant/Award Number: AWS17J012; National Natural Science Foundation of China, Grant/Award Number: 31971028, 31971007

Abstract

Sleep inertia refers to a distinct physiological state of waking up from sleep accompanied by performance impairments and sleepiness. The neural substrates of sleep inertia are unknown, but growing evidence suggests that this inertia state maintains certain sleep features. To investigate the neurophysiological mechanisms of sleep inertia, a comparison of pre-sleep and post-sleep wakefulness with eyes-open resting-state was performed using simultaneous EEG-fMRI, which has the potential to reveal the dynamic details of neuroelectric and hemodynamic responses with high temporal resolution. Our data suggested sleep-like features of slow EEG power and decreased BOLD activity were persistent during sleep inertia. In the pre-sleep phase, participants with stronger EEG vigilance showed stronger activity in the fronto-parietal network (FPN), but this phenomenon disappeared during sleep inertia. A time course analysis confirmed a decreased correlation between EEG vigilance and the FPN activity during sleep inertia. This simultaneous EEG-fMRI study advanced our understanding of sleep inertia and revealed the importance of the FPN in maintaining awareness. This is the first study to reveal the dynamic brain network changes from multi-modalities perspective during sleep inertia.

KEYWORDS

EEG vigilance, fronto-parietal network, resting-state, simultaneous EEG-fMRI, sleep inertia

1 | INTRODUCTION

Sleep inertia is a phenomenon of temporary hypo-vigilance, confusion, disorientation of behavior, and impaired cognitive and behavioral performance right after awakening (Tassi & Muzet, 2000). This awakening state is paradoxical because people may think they are refreshed from the recovery sleep but are in actual fact affected by its negative impact. Previous studies have confirmed various cognitive impairments during sleep inertia, such as response latency (Splaingard, Hayes, & Smith, 2007), error-monitoring function (Asaoka et al., 2010), working memory (Groeger, Lo, Burns, & Dijk, 2011), and decision-making (Bruck & Pisani, 1999). At the extreme, the effect of sleep inertia may be more serious than a night of sleep deprivation, especially when individuals are requested to make vital decisions or take immediate action upon awakening. The state of sleep inertia suggests that re-establishment of vigilance and complex processes underlying consciousness take time to recover. The affected cognitive-behavioral performances reflect loss of functional segregation of large-scale brain networks during this transition state (Vallat, Meunier, Nicolas, & Ruby, 2019). Despite the increasing attention paid to the transition state from wakefulness to sleep over the past 20 years, the phenomenon of awakening from sleep remains largely understudied.

There are at least three neurophysiological interpretations of sleep inertia. First, the brain has different recovery delays for the neocortex and deep brain structures. Upon waking, blood flow increases first in subcortical regions such as the brainstem and thalamus, and subsequently in the frontal lobes (Balkin et al., 2002). These increases result in a rapid re-establishment of basic consciousness followed by slow re-establishment of full awareness. Second, sleep inertia is usually accompanied by microsleep, which is a temporary episode of sleep with increased slow-wave activity. Using electroencephalography (EEG) measurements, several studies have revealed persistent slow waves during sleep inertia (Ferrara et al., 2006; Marzano, Ferrara, Moroni, & De Gennaro, 2011). Detailed analyses of topographical distribution further uncovered predominantly increased slow-wave activity in posterior brain regions (Marzano et al., 2011). Third, from the perspective of functional integration in the brain, sleep inertia is related to the reduced functional connectivity among large-scale brain networks. A global loss of anti-correlation between the task-positive (dorsal attention, salience, sensorimotor) and the task-negative (default mode) networks upon awakening was reported by Vallat et al. (2019). Besides, Tsai and colleagues found decreased functional connectivity within the sensory-motor network upon awakening, revealing the neural underpinning of the poor motor performances during sleep inertia (Tsai et al., 2014).

Previous studies have reported on the relationship between the default mode network (DMN) and dorsal attention network (DAN) at various levels of vigilance and consciousness (Krause et al., 2017; Samann et al., 2011). In light sleep, the anti-correlation between the DMN and DAN was decreased (Samann et al., 2011), and this tendency persisted through wakefulness after partial or total sleep deprivation (De Havas, Parimal, Soon, & Chee, 2012). Recently, Vallat and colleagues (2019) found that the anti-correlation between the DMN and DAN decreased during sleep inertia, indexing disrupted brain function in a variety of contexts. Moreover, an anti-correlation was observed between the DMN and fronto-parietal network (FPN). With a growing body of literature suggesting that the FPN plays a crucial role in regulating the DMN and DAN activities (Gao & Lin, 2012; Spreng, Sepulcre, Turner, Stevens, & Schacter, 2013), our goal is to explore the importance of the FPN in cognitive control during sleep inertia.

Though Vallat et al. and Tsai et al. both collect the simultaneous EEG-fMRI data of pre-sleep and sleep inertia phase, Vallat et al. analyzed the EEG and fMRI data separately (Vallat et al., 2019), while Tsai et al. focused only on fMRI activity and functional connectivity (Tsai et al., 2014). The relationship between EEG vigilance and fMRI activity remains unknown during sleep inertia. More importantly, by using simultaneous EEG-fMRI, dynamic interactions of neuroelectric and hemodynamic responses can be revealed by a time course analysis with high temporal resolution. Hence, BOLD responses of EEG measurements could be clarified with EEG-informed fMRI analyses (Abreu, Leal, & Figueiredo, 2018). To date, a joint analysis of both techniques is lacking in exploring brain network correlates with time-changing EEG upon awakening. This analysis may provide fundamental insight into the nature of sleep inertia from a multimodal perspective.

In this work, we sought to fill the gap of single modality by using the simultaneous recording. Specifically, we gathered resting-state brain functional data with simultaneous EEG-fMRI during pre-sleep and sleep inertia phases. Our first aim was to examine whether sleep-specific features intrude into sleep inertia phase. We hypothesized that sleep-specific features such as increased EEG slow-wave and decreased fMRI activity would persist during this phase. Next, we aimed to explore the link between EEG vigilance and fMRI activity during sleep inertia. Therefore, an EEG-informed fMRI analysis was used to explore whether the fluctuations of the three brain networks (DMN, DAN, and FPN) correlated with electrophysiological temporal dynamics, focusing specifically on the EEG vigilance.

2 | MATERIALS AND METHODS

2.1 | Participants

A total of 108 participants, aged between 18 to 25 years (mean ± SD: 21.27 ± 1.71 years, 56 males/52 females) were recruited through online advertisement. No history of psychiatric or neurological illness was reported. No alcoholic or caffeinated food or drink was allowed on the testing date. The Pittsburgh Sleep Quality Index (PSQI) was administered to all participants to examine their sleep quality in the previous month. Self-rating depression scale (SDS) and self-rating anxiety scale (SAS) were tested before scanning. There were 53 participants quit the experiment after the adaptive sleep, because of failing to fall asleep in the noise and narrow MRI scanner. Hence, 55 participants took part in the formal experiment. Each participant was paid 120 CNY after completion of the study. This study was approved by the Review Board of the Institute of Southwest University. Written informed consent was obtained after a detailed explanation of the study protocol. All experiments were in accordance with the Declaration of Helsinki.

2.2 | Procedures

Participants arrived at the Sleep and Neuroimaging Center at Southwest University around 11 p.m. Upon arrival, an MRI-compatible EEG cap was set up for later recording of (a) pre-sleep phase (5 min), (b) sleeping phase (2 hr), and (c) sleep inertia phase (5 min). We checked the impedance before each phase and made sure the impedance was below 10 kΩ. Simultaneous EEG–fMRI recordings were conducted for all the three phases. During both pre-sleep and sleep inertia phases, participants viewed a fixation point on the screen, relaxed, and were told to not consciously think of anything. In the sleeping phase, participants slept without lights and were awakened by calling their first name. Experiment was conducted between 11 p.m. in the first night and 4 a.m. in the next morning. During pre-sleep and sleep inertia phases, the participants were told to stay awake and not to fall asleep. This was important in our study because we focused on the pre-sleep and sleep inertia waking states.

2.3 | Acquisition of EEG data

A 32-channel MRI-compatible Brain Products system was utilized for EEG recording (BrainAmp MR plus, Brain Products, Munich, Germany). The cap was set based on the international 10/20 system. Impedance was adjusted below 10 kΩ. FCz was taken as reference, and the sampling rate was 5 kHz. To guarantee the temporal stability of acquisition relative to switching of the gradients in scanning, a SyncBox (SyncBox MainUnit, Brain Products GmbH, Munich, Germany) was used to synchronize the amplifier system. The amplified and digitized EEG signal was transmitted to the recording computer placed outside the scanner room via a fiber optic cable.

2.4 | Neuroimaging acquisition

Whole-brain resting-state BOLD signals were acquired using a 3 T Siemens Trio scanner. A total of 200 functional volumes were obtained in each period with a T2-weighted gradient echo-planar imaging (EPI) sequence (repetition time [TR]/echo time [TE] of 1500/29 ms, field of view [FOV] of 192×192 mm^2, flip angle of 90°, acquisition matrix of 64×64, thickness/gap of 5/0.5 mm, in-plane resolution of 3.0×3.0 mm^2, axial slices of 25). Acquisition of structural images (T1) continued for 5 min with the 3D-SPGR sequence (TR/TE of 8.5/3.4 ms, FOV of 240×240 mm^2, flip angle of 12°, acquisition matrix of 512×512, thickness/gap of 1/0 mm), providing an anatomical template for the functional scan. A cushioned head fixation device was used to minimize head movements.

2.5 | Sleep staging

Before sleep staging, EEG signals were corrected by removing artifacts (see details in EEG data analysis section below). Six channels (F3, F4, C3, C4, O1, O2) were selected and montaged for manual sleep staging. Two authors (XC and XL) scored the EEG signal with a time window of 30 s, according to the 2017 AASM manual (Berry et al., 2017). For the inconsistent epochs, a light sleep stage was accepted. A total of 43 participants who have the time of continuous N3 sleep longer than 5 min during sleeping phase were analyzed. The recordings from 12 participants were discarded from further analyses.

2.6 | EEG data analysis

Following the standard template subtraction method, we first removed the fMRI gradient and ballistocardiographic artifacts from the original EEG recording (Allen, Josephs, & Turner, 2000). Then, the EEG signals were down-sampled to 250 Hz and digitally filtered within the 0.1–45 Hz frequency band using a Chebyshev II-type filter. From the EEG data, it was easy to identify the ocular artifacts associated with blinking, and this confirmed the success of experimental manipulation of eyes-open resting-state recording. Temporal independent component analysis (ICA) was performed to further eliminate the residual fMRI gradient and ballistocardiographic, ocular, and muscle activity artifacts. The filtered EEG signals were re-referenced to average references for further analyses. All steps were performed within Brain Vision Analyzer software (Version 2.0, Brain Products, Inc., Munich, Germany).

The artifact-corrected EEG signal was segmented to 3 s, corresponding to two TR of our fMRI acquisition. Using a fast Fourier transform (FFT), we calculated the power in three frequency bands: delta (1–4 Hz), theta (4–7 Hz), and alpha (8–13 Hz). The power value was transformed into logarithms ($10 \times \log_{10}[\mu v^2/\text{Hz}]$) to approximate a normal distribution. This resulted in three time series and each represented one frequency band, with time points of 100 (i.e., 300 s). The EEG vigilance was calculated as the ratio between the power of alpha band and the average power of theta and delta bands (Wong, Deyoung, & Liu, 2016; Wong, Olafsson, Tal, & Liu, 2013), and was transformed into logarithms.

2.7 | Neuroimaging data analyses

The data was preprocessed using SPM12 (http://www.fil.ion.ucl.ac.uk/spm/, Welcome Department of Cognitive Neurology, University College London, UK), including preprocessed pipeline of realignment, slice timing, head motion correction, segmentation, coregistration, spatial normalization, and smoothing. The head motion of each participant was not allowed to exceed 3 mm or 3°. The group ICA was applied with the GIFT toolbox (http://icatb.sourceforge.net/)(Calhoun, Adali, Pearlson, & Pekar, 2001) to extract resting-state networks. We selected 25 as the optimal number of components, which was estimated using the minimum description length criterion (Li, Adali, & Calhoun, 2007). Before ICA, data reduction was conducted with principal component analysis (PCA). The analyses of ICA decomposition were implemented on concatenated datasets using the Extended Infomax algorithm. Time courses and spatial patterns of each participant were reconstructed, and the mean spatial maps of each group were transformed to z-scores for display purposes.

The DMN, DAN, and FPN maps from a previous fMRI study of resting-state were employed (Lei, Zhao, & Chen, 2013) as spatial templates for component identification. Based on the templates, the selected brain networks corresponded to those components with the largest spatial correlations. In addition, these correlations showed at least twofold stronger correlation values than other networks. Figure 1 presents the spatial anatomy of the three networks. Anatomical locations with the corresponding Montreal Neurological Institute (MNI) coordinates (Tzourio-Mazoyer et al., 2002) are listed in Table 1.

After ICA analyses, the constrained minimal lagged correlation was conducted with the FNC toolbox (http://mialab.mrn.org/software/#fnc,) (Jafri, Pearlson, Stevens, & Calhoun, 2008; Xin & Lei, 2015) to measure interactions of the three networks. Pearson correlations among extracted time courses of functional connectivity from the DMN, DAN, and FPN networks of each participant were calculated. The obtained correlation coefficients were transformed into normally distributed values using Fisher's r-to-z transformation. Paired t-tests were employed to compare the functional connectivity between pre-sleep and sleep inertia phases.

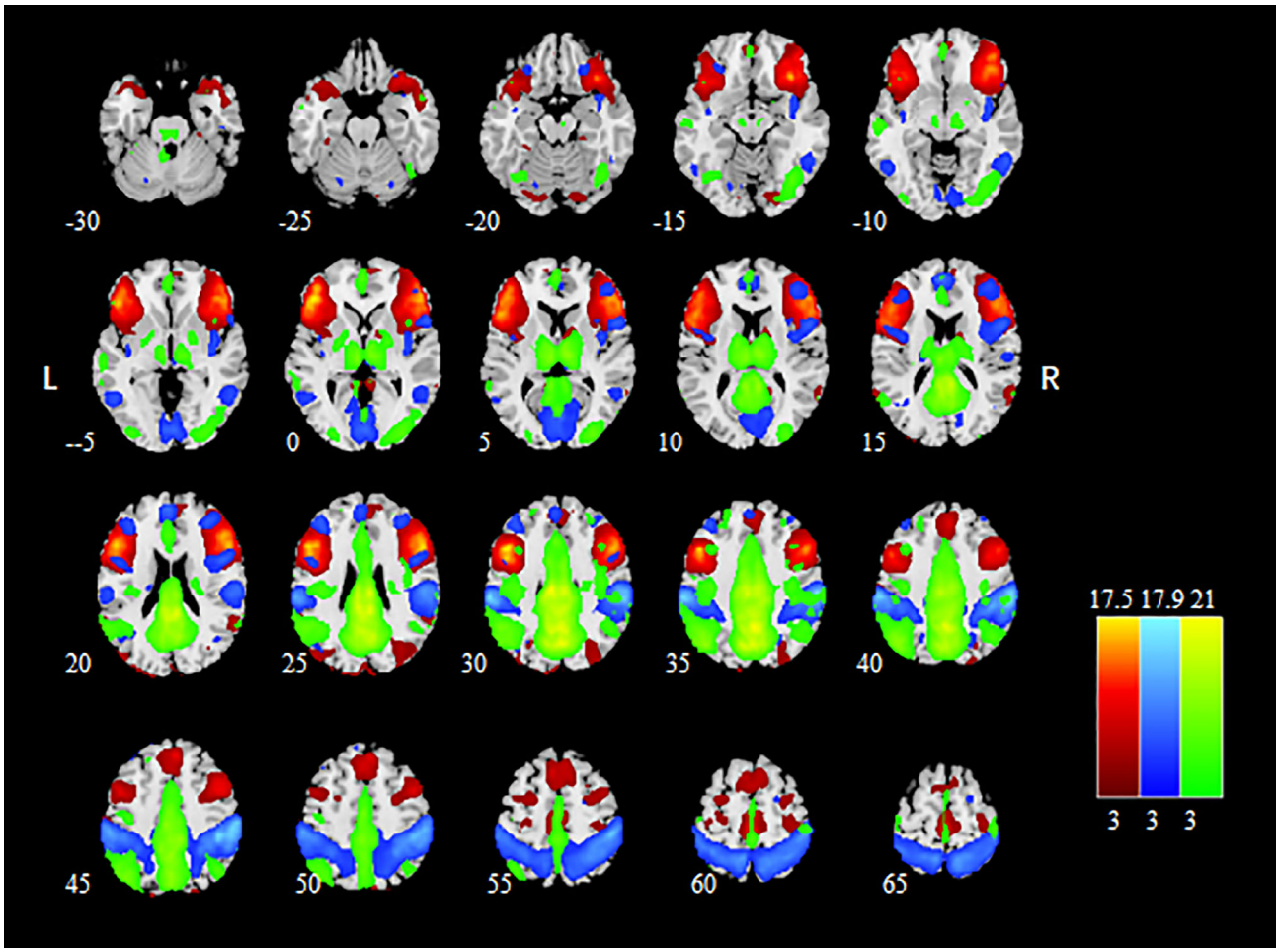

FIGURE 1 The spatial distribution of the DMN, DAN, and FPN. Brain areas with intensities of two SD greater than the mean are shown. DMN, default mode network (green); DAN, dorsal attention network (blue); FPN, fronto-parietal network (red)

Based on the time courses of each component, the low-frequency fluctuation (ALFF, the average amplitude of power between 0.01 and 0.1 Hz) in each condition was calculated. This is based on FFT, and power is calculated by computing the area under the spectrum curve (Zang et al., 2007). Notice that because our data is original data scaled using intensity normalization, the ALFF has arbitrary unit. However, this value is comparable between sessions and across participant, because the time courses of each participant in each session were back-reconstruction from the same IC of a brain network. More details about the back-reconstruction process of group ICA can be found in (Calhoun et al., 2001).

2.8 | Correlation between EEG vigilance and time courses of brain networks

For time course analysis in individual-level, some crucial steps to obtain the EEG vigilance and fMRI time course were displayed in Figure 2. The time course of EEG vigilance of all channels was averaged to obtain the whole brain EEG vigilance. Because of the low signal-to-noise ratio, the time points of outliers were removed and replaced by linear interpolating method using Matlab function interp1. The removed outliers had distances 2.5 times larger than the *SD*, and the distances were defined as the absolute value between the power value and median value of each time series. The number of removed time points for each participant ranged from 3 to 25 (mean ± *SD* = 12.3 ± 4.8). Considering the neuro-vascular relationship, the averaged EEG vigilance was further convolved with the standard hemodynamic response function (HRF). The final curve of EEG vigilance was correlated with the time course of the three brain networks.

For group-level analysis, the correlation coefficients of each participant were calculated and were normalized by Fisher's r-to-z method. A one-sample *t*-test analysis was conducted to examine the validity of the correlation between EEG vigilance and fMRI time course of each network.

3 | RESULTS

3.1 | Demographic and questionnaire data

Details of participants' demographic variables and cross-correlations of questionnaire scores are summarized in Table 2. All participants were good sleepers (PSQI <7). No symptoms of depression (SDS < 61) or anxiety (SAS < 59) were observed. In total, 43 participants reached slow-

TABLE 1 Peak foci for the DMN, DAN, and FPN defined by group ICA

Regions	MNI coordinates			T
	X	Y	Z	
DMN				
R precuneus	3	−57	36	21.20
R post cingulum	6	−42	21	19.94
L angular	−42	−72	36	12.73
R middle occipital gyrus	33	−93	6	8.45
R inferior occipital gyrus	30	−93	−6	6.04
DAN				
R supramarginal gyrus	60	−30	36	18.31
L supramarginal gyrus	−63	−27	33	16.58
L medial frontal gyrus	−3	57	18	9.26
R calcarine sulcus	3	−75	3	8.70
R midcingulate area	12	−30	42	8.45
R middle frontal gyrus, orbital part	51	9	21	7.38
L middle frontal gyrus	−39	42	36	6.68
FPN				
L inferior frontal gyrus, pars opercularis	−48	18	33	19.63
R inferior frontal gyrus, pars triangularis	54	21	24	16.68
R medial frontal gyrus	6	42	45	9.57
L paracentral lobule	0	−24	57	9.52
Lobule IV, V of vermis	6	−45	3	6.68

Abbreviations: DAN, dorsal attention network; DMN, default mode network; FPN, fronto-parietal network; L, left; R, right.

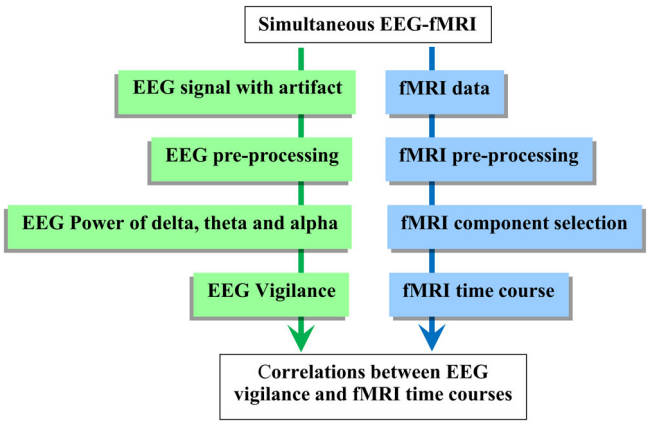

FIGURE 2 A flow diagram of correlation analyses between EEG vigilance and fMRI time courses. EEG and fMRI signals were processed with the model-specific methods and were correlated in the temporary domain. Original EEG data were correlated with the fMRI gradients and ballistocardiographic artifacts. Then, frequencies of delta, theta, and alpha band powers were calculated, and the EEG vigilance was estimated. For fMRI signals, group ICA was conducted. Brain networks, including the DMN, DAN, and FPN, were selected. The correlations were calculated between fMRI time courses of brain networks and EEG vigilance, which was convoluted with the hemodynamic response function to obtain the predictor of BOLD responses. DMN, default mode network; DAN, dorsal attention network; FPN, fronto-parietal network

wave sleep in the sleeping phase (mean N3 sleep time = 39.03 min, *SD* = 23.55). With regard to the main sleep stage of the last 5 min before awakening, 44.2% of participants awoke from N2 sleep and 27.9% from N3 sleep. A negative correlation between SDS score and slow-wave sleep time ($r = -0.404$, $p = .007$) was observed, consistent with a previous report that people with depressive tendencies often suffer from more sleep disturbances (Horvath et al., 2015).

3.2 | Increased EEG power of delta band

EEG powers between pre-sleep and sleep inertia were compared using paired t-tests (Figure 3a). Increased delta power during sleep inertia ($t_{(42)} = 2.23$, $p = .015$) was observed. However, neither the frequencies of alpha nor theta band power reached significance in comparison between the pre-sleep and sleep inertia phases. The EEG vigilance was not significant ($t_{(42)} = 1.28$, $p = .105$) between the two phases, although the value implied decreased vigilance (mean = 5.87 vs. mean = 6.77) during sleep inertia phase.

3.3 | Altered fMRI brain networks

Based on the time courses of each network, the low-frequency fluctuation (ALFF, the average amplitude of power between 0.01 and

TABLE 2 Demographic and questionnaire data, and cross-correlations between parameters

Measure	Mean	*SD*	Correlation with	SAS	SDS	PSQI	N3 sleep
Age	21.07	1.549		0.093	0.060	0.098	−0.076
BMI	21.23	3.443		−0.235	−0.123	0.091	−0.044
SAS	38.26	6.616		1	0.624**	0.170	−0.276
SDS	42.81	6.507			1	0.248	−0.404*
PSQI	4.64	1.511				1	0.068
N3	39.03	23.553					1

Abbreviations: BMI, body mass index; N3, duration of N3 sleep (min), that is, time of slow-wave sleep; PSQI, Pittsburgh Sleep Quality Index; SAS, self-rating anxiety scale; *SD*, standard deviation; SDS, self-rating depression scale.
*p < .01, **p < .001.

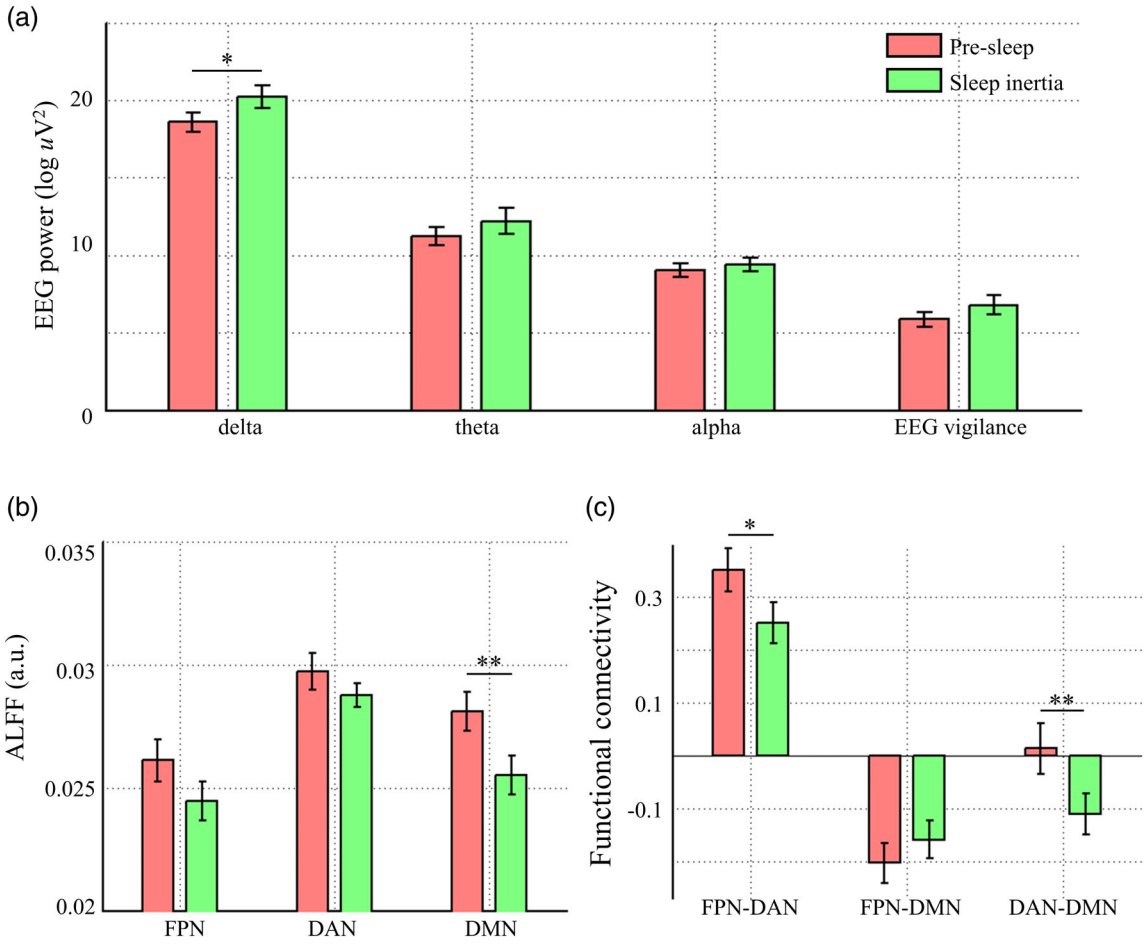

FIGURE 3 Comparisons of EEG rhythms and fMRI brain networks during pre-sleep (red) and sleep inertia phases (green). (a). EEG rhythms and EEG vigilance during pre-sleep and sleep inertia phases. (b). The low-frequency fluctuation (ALFF) of the DMN, DAN, and FPN. (c). The functional connectivity among the three brain networks. DMN, default mode network; DAN, dorsal attention network; FPN, fronto-parietal network
*p < .05, **p < .01

0.1 Hz (Zang et al., 2007)) in the pre-sleep and sleep inertia phases was compared in the three networks (Figure 3b). Notably, the spontaneous activity of the DMN was significantly decreased during sleep inertia ($t_{(42)}$ = 2.787, p = .003). This decrease was also observed in the FPN ($t_{(42)}$ = 1.525, p = .067) and DAN ($t_{(42)}$ = 1.214, p = .115) but did not reach significance.

Functional connectivities among these three networks are illustrated in Figure 3c. During sleep inertia, the DMN-DAN connectivity

and FPN-DAN connectivity were significantly decreased ($t_{(42)}$ = 2.910, p = .005 and $t_{(42)}$ = 2.031, p = .048, respectively). The FPN-DMN connectivity showed no significant change between the two phases ($t_{(42)}$ = −1.105, p = .275).

3.4 | EEG-fMRI fusion

Based on simultaneous EEG-fMRI, a temporal correlation analysis was conducted between the EEG vigilance and time courses of fMRI brain networks at the individual level. In Figure 4a, a negative correlation was observed between the EEG vigilance and fMRI signals of the FPN (r after fish-z-transform: −0.140 ± 0.256, p < .001). However, this correlation disappeared during sleep inertia (r after fish-z-transform: 0.018 ± 0.244, p = .313). An illustration of this phenomenon for one participant (No. 7) is shown in Figure 4b,c. Here, for ease of visualization, an inverted wave of EEG vigilance is plotted. A high correlation coefficient (r = −0.329, p < .001) was observed in the pre-sleep phase (Figure 4b), while this correlation (r = −0.037, p = .602) was disappeared during sleep inertia (Figure 4c). This phenomenon was not observed for the other two networks, that is, the DAN (pre-sleep: 0.012 ± 0.272; sleep inertia: 0.028 ± 0.221) and DMN (pre-sleep: 0.077 ± 0.260; sleep inertia: 0.032 ± 0.268). In short, our data illustrated that the FPN lost its strong correlation with the EEG vigilance during sleep inertia.

To further investigate the relationship between the EEG vigilance and fMRI fluctuations, a group-level correlation analysis was performed. Differences between pre-sleep and sleep inertia phases in the EEG vigilance and ALFF of each brain network were calculated for each participant. Pearson correlations between the EEG vigilance and ALFF of each brain network were calculated. Notably, the correlations were conducted by using the different values between pre-sleep and sleep inertia. A positive correlation between the EEG vigilance and ALFF of the FPN was observed (r = 0.327, p = .032, Figure 5a). No correlation was detected in the DAN (r = 0.179, p = .250, Figure 5b) or DMN (r = 0.117, p = .456, Figure 5c).

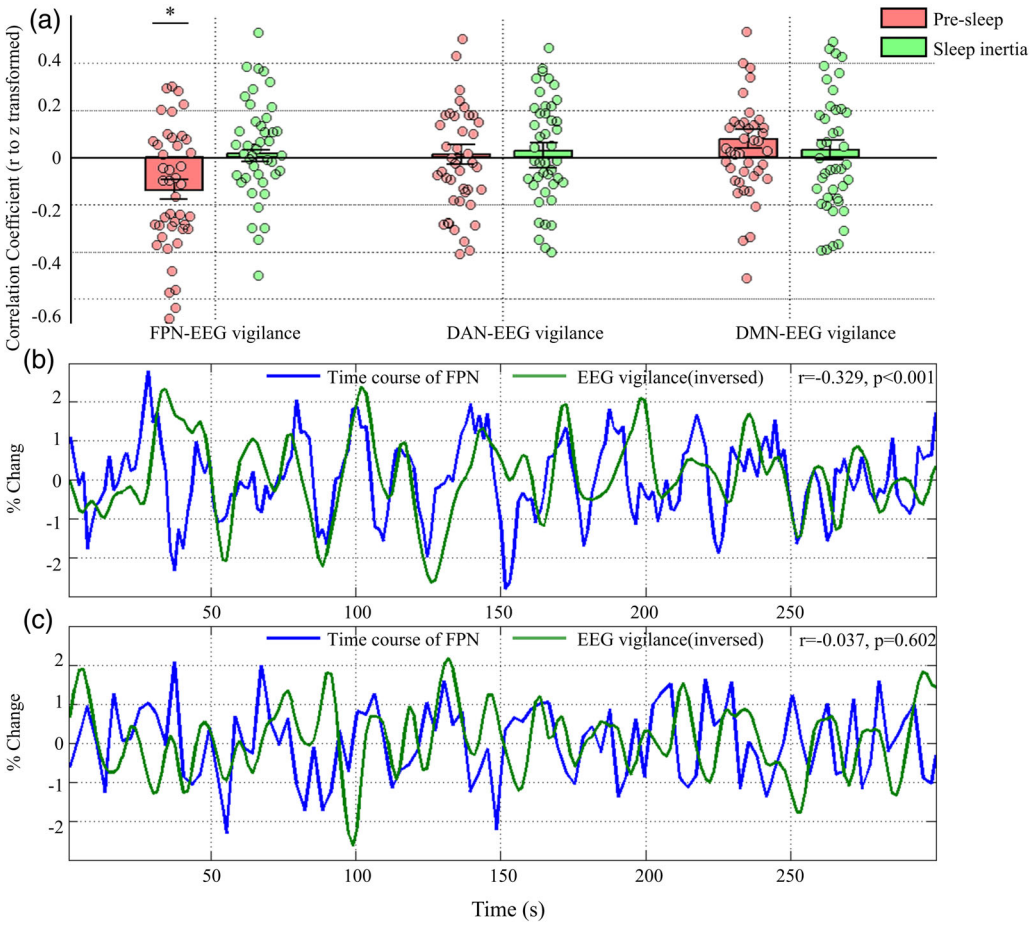

FIGURE 4 Correlation between EEG vigilance and time course of resting-state networks. (a). The mean and *SE* of the correlation between EEG vigilance and three networks during pre-sleep (red) and sleep inertia (green) phase. Each dot represents one participant. (b). Relationship between EEG vigilance and time course of the FPN in one participant during pre-sleep resting-state. (c). Relationship between EEG vigilance and time course of the FPN in the same participant during sleep inertia. Blue line: time course of fMRI brain network; green line: EEG vigilance. Note that the EEG vigilance was inverse plotted (i.e., multiply with −1) for ease of visualization. DMN, default mode network; DAN, dorsal attention network; FPN, fronto-parietal network

* p<0.01

4 | DISCUSSION

In the present study, we investigated the relationship between EEG power and brain networks during sleep inertia using simultaneous EEG-fMRI. An important finding was that some sleep features were intrusive into sleep inertia and were reflected by EEG signals and fMRI images. For EEG, both increased power of delta band and decreased EEG vigilance were observed, although the latter was not significant. For fMRI, both brain activity and functional connectivity were decreased for the three large-scale networks. More importantly, the FPN lost its regulation of EEG vigilance upon awakening; the neural substrate underpinning this phenomenon was the impaired dynamic interaction revealed by simultaneous EEG-fMRI. Our data provides new multimodal neurophysiological evidence of sleep inertia.

Our findings shed light on the brain networks correlated with slow EEG patterns during sleep inertia. The simultaneous EEG-fMRI measurement allows investigation of the correlation of BOLD signals with the power fluctuation of EEG in specific frequency bands over time. Previous studies only reported the increased slow waves upon awakening, but the neural mechanisms of intruding sleep-like EEG characteristics remain uncertain. The diminished anti-correlation between the EEG vigilance and BOLD signal of the FPN with time scale of single fMRI TR may indicate complex temporal dynamics upon awakening, which could help to illuminate the neural mechanisms of sleep inertia.

4.1 | Increased EEG power of delta band

Compared to pre-sleep wakefulness, the power of EEG delta band was increased ($t_{(42)}$ = 2.23, p = .015) during sleep inertia, which was in accordance with previous studies (Ferrara et al., 2006; Marzano et al., 2011; Trotti, 2017). As the power of delta band is a marker of deep sleep, our results concurred with the opinion that sleep inertia is not only a result of residual EEG features of sleep intruding into awakening, but is also a confirmation of microsleep. Moreover, the emergence of delta power may represent the intrinsic bistability of cortical networks, suggesting a transition between hyperpolarized (down) states and depolarized (up) states (Tononi, Massimini, & Riedner, 2006). In our study, the increased delta power during sleep inertia may characterize the cortical bistability during waking process.

4.2 | Decreased activity and functional connectivity of brain networks

Decreased activities of the three networks were observed upon awakening, especially the DMN ($t_{(42)}$ = 2.787, p = .003), suggesting deficient vigilance during sleep inertia. This linkage of diminished vigilance and reduced spontaneous activity of the DMN has also been reported in previous studies (Dai et al., 2015; Song et al., 2017). Furthermore, lower BOLD activity in the DMN indicated reduced vigilance and worse performance (Gui et al., 2015). These results were consistent with reports of reduced DMN activity in decreased consciousness, such as deep sleep (Tagliazucchi & van Someren, 2017), consciousness disorders (Laureys, 2005), and anesthesia (MacDonald, Naci, MacDonald, & Owen, 2015). Collectively, the decreased DMN activity during sleep inertia in the current study suggested the partial loss of conscious awareness upon awakening. This loss of consciousness was compared to the pre-sleep phase in which participants had high conscious awareness. This result also confirmed Tsai's work which found the ALFF decreased in the posterior brain regions after sleep (Tsai

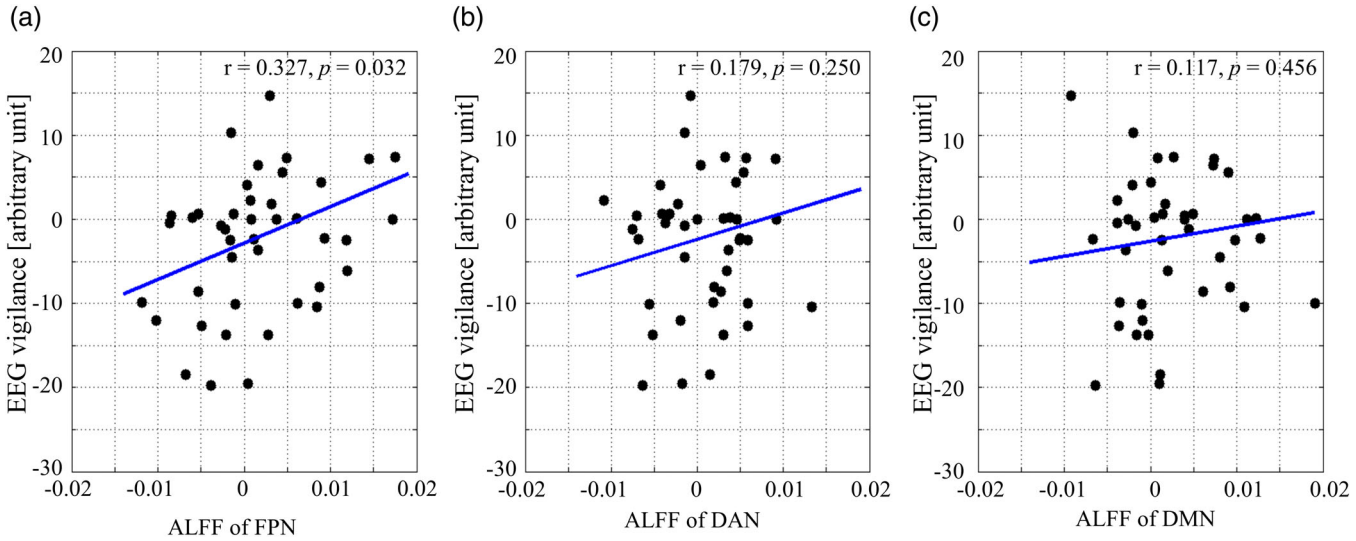

FIGURE 5 Correlation between the EEG vigilance and ALFF of the three brain networks at a group level. All values indicate the differences between pre-sleep and sleep inertia phases. (a). Correlation between the EEG vigilance and ALFF of the FPN. (b). Correlation between the EEG vigilance and ALFF of the DAN. (c). Correlation between the EEG vigilance and ALFF of the DMN. DMN, default mode network; DAN, dorsal attention network; FPN, fronto-parietal network

et al., 2014). The tendency for decreased activity of task-positive networks (the FPN and DAN) indicated the persistence of sleep features and may provide a neurophysiological explanation for the impaired behavioral performance during sleep inertia. Previous studies have revealed the decreased activity of task-positive networks during deep sleep (Kaufmann, 2006) and the increased activity during various cognitive tasks. The overall decreased activity in the three networks implied inactive and low vigilance of the brain during sleep inertia.

Our findings demonstrated that the anti-correlation of functional connectivity between the DAN and DMN was strengthened during sleep inertia. This was inconsistent with a previous study (Vallat et al., 2019). The difference may be due to different scanning time. In the previous study, the scanning time was in the afternoon (1 p.m. to 3 p.m.); however, we conducted our study around midnight (11 p.m. to 4 a.m.). The increased anti-correlation may reflect a compensatory mechanism occurring due to our participants struggling with staying awake under the dual effect of sleep inertia and circadian rhythm. In contrast, the connectivity between the FPN and DAN decreased upon awakening. The FPN selectively augments or suppresses the DMN and DAN depending on the task demand (Xin & Lei, 2015). Specifically, the FPN exhibited a high positive correlation with the DAN during externally focused goal-directed cognition (Gao & Lin, 2012). Thus, the decreased FPN-DAN correlation may indicate an unresponsive brain state during sleep inertia. Our results suggested that the key issue of sleep inertia is dependent on decreased absolute connectivity from the FPN to DMN and DAN, rather than decreased DMN-DAN connectivity (Vallat et al., 2019).

4.3 | The neurophysiological mechanisms of sleep inertia

The main finding of the current study was the loss of frontal area control of EEG vigilance during sleep inertia. Specifically, during pre-sleep wakefulness, there was a negative correlation between EEG vigilance and spontaneous fluctuation of the FPN (z-transformed r: −0.140 ± 0.256, $p < .001$). However, there was no correlation during sleep inertia (z-transformed r: 0.018 ± 0.244, $p = .313$). This finding was observed both at the single-subject and group level (see Figures 4 and 5).

The brain substrates of vigilance mainly encompass frontal, parietal, and thalamic areas (Coull, Jones, Egan, Frith, & Maze, 2004; Shaw et al., 2009). Previous studies have indicated that the increased activity of the FPN with the occurrence of pupil dilation (Schneider et al., 2016) and microsleep (Poudel, Innes, & Jones, 2018) after sleep deprivation, indicating top-down control following a transient decrease in vigilance. The pre-sleep resting-states of participants were scanned at 1 a.m. to be analogous to the sleep deprivation state, as they were under high sleep pressure at this time point. It has been reported that the response of the fronto-parietal region to a vigilance task was reduced after sleep deprivation for a night (Poudel, Innes, & Jones, 2013). Another study indicated that vigilance lapses (failures) were related to the reduced activation in the FPN (Chee et al., 2008). Thus, during presleep wakefulness, a negative correlation between EEG vigilance and FPN time course emerged, suggesting a role of the FPN in maintaining wakefulness under sleep pressure.

During the slow and gradual process of awakening, the correlation between the FPN activity and the time course of EEG vigilance diminished. This finding was consistent with that of Balkin et al. (2002), in which the prefrontal area played a key role in alertness to re-start the feeling of awakening from sleep. One possible explanation for the diminishing relationship is that, during sleep inertia, EEG vigilance may be mediated by subcortical regions rather than the FPN. The awakening process is mediated via top–down cortical activation of the reticular activation system (RAS), covering numerous projections from the brainstem to cerebral cortex (Magoun, 1952). Further, fluctuations in RAS neuronal firing frequency require time to convert to variation in cortical excitability. We thus speculated that subcortical regions may regulate EEG vigilance upon awakening.

An alternative interpretation is the low acetylcholine level during sleep inertia. The activity of the cholinergic system reaches its lowest level during slow-wave sleep (Diekelmann & Born, 2010); and this phenomenon continues upon awakening. In fact, cholinergic inputs to the fronto-parietal cortex have been related to performance in selective and sustained attention tasks (Arnold, Burk, Hodgson, Sarter, & Bruno, 2002). Acetylcholine release is high when individuals face tasks demanding high attention(Himmelheber, Sarter, & Bruno, 2000). Therefore, the diminished anti-correlation between the FPN and EEG vigilance may result from the low acetylcholine level upon awakening.

4.4 | Limitation

Our simultaneous EEG-fMRI study of sleep inertia provided insight into the possible link between EEG vigilance and activity of brain networks. However, it is important to note that our study has several limitations. First, due to irregular head movement during sleep, there were many artifacts in the sleep EEG data, which may lead to inaccurate sleep staging. The main influence was our statistic parameter of N3 sleep. Due to this technical consideration, our EEG data during the awake stage were also contaminated. In our current study, average artifact subtraction and ICA were both employed to eliminate artifacts. Given that similar artifacts existed both in pre-sleep and sleep inertia phases and we focused on the differences between both phases, the error caused by this problem was small. However, caution must be exercised when extending our results. Second, we lacked a behavioral index to measure the intensity of sleep inertia. The psychomotor vigilance test (PVT) test is widely utilized to measure vigilance. Future studies should consider this test to add a behavioral measure of sleep inertia. Third, since we only collected 5-min sleep inertia data, we could not investigate the dynamic recovery of consciousness from sleep inertia effect. Future studies could consider collecting multiple post-sleep data to explore the dissipation of sleep inertia. Fourth, due to our participants are from a very constrained age group, caution must be exercised when extending our results to a broader age group. Future research can consider investigating the age effect of sleep

inertia. Finally, our experiment was conducted between 11:00 p.m. and 4:00 a.m. in night. Although the inertia effect was strong, this condition is rarely encountered in real life. A more ecological validity design would be to scan participants during the morning, immediately after waking.

5 | CONCLUSION

Using simultaneous EEG-fMRI, we confirmed that sleep inertia is accompanied by sleep-specific brain activity, including higher EEG delta activity and smaller spontaneous BOLD fluctuations. In addition, the functional connectivity among large-scale networks was decreased, revealing a functional separation of the whole brain network. More importantly, the strong correlation between the EEG vigilance and time course of the fronto-parietal network was lost during sleep inertia. Our results revealed that sleep inertia is mostly related to the loss of frontal control of vigilance, which reasonably explained both the EEG and fMRI phenomena. This is the first study to reveal the fMRI brain networks related to the dynamics of EEG vigilance during sleep inertia. Our results provide insight into this common brain state and may facilitate development of potential treatments for sleep disorders related to jet lag and shift work.

ACKNOWLEDGMENTS

The authors thank Yulin Wang, Xiaoli Huang, and Xiaoyong Wan for substantial help in data collection. This work was supported by the National Science Foundation of China (grant number 31971028, 31971007) and Major Project of Medicine Science and Technology of PLA (AWS17J012).

CONFLICT OF INTEREST

The authors declare no conflict of interest.

DATA AVAILABILITY STATEMENT

The datasets used in this study are not shared.

ORCID

Xinyuan Chen https://orcid.org/0000-0002-5866-4665
Xu Lei https://orcid.org/0000-0003-2271-1287

REFERENCES

Abreu, R., Leal, A., & Figueiredo, P. (2018). EEG-informed fMRI: A review of data analysis methods. *Frontiers in Human Neuroscience*, *12*, 29. https://doi.org/10.3389/fnhum.2018.00029

Allen, P. J., Josephs, O., & Turner, R. (2000). A method for removing imaging artifact from continuous EEG recorded during functional MRI. *Neuroimage*, *12*(12), 230–239. https://doi.org/10.1006/nimg.2000.0599

Arnold, H. M., Burk, J. A., Hodgson, E. M., Sarter, M., & Bruno, J. P. (2002). Differential cortical acetylcholine release in rats performing a sustained attention task versus behavioral control tasks that do not explicitly tax attention. *Neuroscience*, *12*(2), 451–460.

Asaoka, S., Masaki, H., Ogawa, K., Murphy, T. I., Fukuda, K., & Yamazaki, K. (2010). Performance monitoring during sleep inertia after a 1-h daytime nap. *Journal of Sleep Research*, *19*(3), 436–443. https://doi.org/10.1111/j.1365-2869.2009.00811.x

Balkin, T. J., Braun, A. R., Wesensten, N. J., Jeffries, K., Varga, M., Baldwin, P., … Herscovitch, P. (2002). The process of awakening: A PET study of regional brain activity patterns mediating the re-establishment of alertness and consciousness. *Brain*, *125*(Pt 10), 2308–2319.

Berry, R. B., Brooks, R., Gamaldo, C., Harding, S. M., Lloyd, R. M., Quan, S. F., … Vaughn, B. V. (2017). AASM scoring manual updates for 2017 (version 2.4). *Journal of Clinical Sleep Medicine*, *13*(5), 665–666. https://doi.org/10.5664/jcsm.6576

Bruck, D., & Pisani, D. L. (1999). The effects of sleep inertia on decision-making performance. *Journal of Sleep Research*, *8*(2), 95–103.

Calhoun, V. D., Adali, T., Pearlson, G. D., & Pekar, J. J. (2001). A method for making group inferences from functional MRI data using independent component analysis. *Human Brain Mapping*, *14*(3), 140–151.

Chee, M. W., Tan, J. C., Zheng, H., Parimal, S., Weissman, D. H., Zagorodnov, V., & Dinges, D. F. (2008). Lapsing during sleep deprivation is associated with distributed changes in brain activation. *Neuroscience*, *28*(21), 5519–5528. https://doi.org/10.1523/jneurosci.0733-08.2008

Coull, J. T., Jones, M. E., Egan, T. D., Frith, C. D., & Maze, M. (2004). Attentional effects of noradrenaline vary with arousal level: Selective activation of thalamic pulvinar in humans. *NeuroImage*, *22*(1), 315–322. https://doi.org/10.1016/j.neuroimage.2003.12.022

Dai, X. J., Liu, C. L., Zhou, R. L., Gong, H. H., Wu, B., Gao, L., & Wang, Y. X. (2015). Long-term total sleep deprivation decreases the default spontaneous activity and connectivity pattern in healthy male subjects: A resting-state fMRI study. *Neuropsychiatric Disease and Treatment*, *11*, 761–772. https://doi.org/10.2147/ndt.S78335

De Havas, J. A., Parimal, S., Soon, C. S., & Chee, M. W. (2012). Sleep deprivation reduces default mode network connectivity and anti-correlation during rest and task performance. *NeuroImage*, *59*(2), 1745–1751. https://doi.org/10.1016/j.neuroimage.2011.08.026

Diekelmann, S., & Born, J. (2010). The memory function of sleep. *Nature Reviews. Neuroscience*, *11*(2), 114–126. https://doi.org/10.1038/nrn2762

Ferrara, M., Curcio, G., Fratello, F., Moroni, F., Marzano, C., Pellicciari, M. C., & Gennaro, L. D. (2006). The electroencephalographic substratum of the awakening. *Behavioural Brain Research*, *167*(2), 237–244. https://doi.org/10.1016/j.bbr.2005.09.012

Gao, W., & Lin, W. (2012). Frontal parietal control network regulates the anti-correlated default and dorsal attention networks. *Human Brain Mapping*, *33*(1), 192–202. https://doi.org/10.1002/hbm.21204

Groeger, J. A., Lo, J. C., Burns, C. G., & Dijk, D. J. (2011). Effects of sleep inertia after daytime naps vary with executive load and time of day. *Behavioral Neuroscience*, *125*(2), 252–260. https://doi.org/10.1037/a0022692

Gui, D., Xu, S., Zhu, S., Fang, Z., Spaeth, A. M., Xin, Y., … Rao, H. (2015). Resting spontaneous activity in the default mode network predicts performance decline during prolonged attention workload. *NeuroImage*, *120*, 323–330. https://doi.org/10.1016/j.neuroimage.2015.07.030

Himmelheber, A. M., Sarter, M., & Bruno, J. P. (2000). Increases in cortical acetylcholine release during sustained attention performance in rats. *Brain Research. Cognitive Brain Research*, *9*(3), 313–325.

Horvath, A., Szucs, A., Montana, X., Lanquart, J. P., Hubain, P., Flamand, M., … Loas, G. (2015). Individual differences in sleep macrostructure: Effects of anxiety, depression, aging and gender. *Neuropsychopharmacologia Hungarica*, *17*(3), 146–156.

Jafri, M. J., Pearlson, G. D., Stevens, M., & Calhoun, V. D. (2008). A method for functional network connectivity among spatially independent resting-state components in schizophrenia. *NeuroImage*, *39*(4), 1666–1681. https://doi.org/10.1016/j.neuroimage.2007.11.001

Kaufmann, C., Wehrle, R., Wetter, T. C., Holsboer, F., Auer, D. P., Pollmacher, T., & Czisch, M. (2006). Brain activation and hypothalamic

functional connectivity during human non-rapid eye movement sleep: an EEG/fMRI study. *Brain*, *129*(3), 655–667. https://doi.org/10.1093/brain/awh686

Krause, A. J., Simon, E. B., Mander, B. A., Greer, S. M., Saletin, J. M., Goldstein-Piekarski, A. N., & Walker, M. P. (2017). The sleep-deprived human brain. *Nature Reviews. Neuroscience*, *18*(7), 404–418. https://doi.org/10.1038/nrn.2017.55

Laureys, S. (2005). The neural correlate of (un)awareness: Lessons from the vegetative state. *Trends in Cognitive Sciences*, *9*(12), 556–559. https://doi.org/10.1016/j.tics.2005.10.010

Lei, X., Zhao, Z., & Chen, H. (2013). Extraversion is encoded by scale-free dynamics of default mode network. *NeuroImage*, *74*, 52–57. https://doi.org/10.1016/j.neuroimage.2013.02.020

Li, Y. O., Adali, T., & Calhoun, V. D. (2007). Estimating the number of independent components for functional magnetic resonance imaging data. *Human Brain Mapping*, *28*(11), 1251–1266. https://doi.org/10.1002/hbm.20359

MacDonald, A. A., Naci, L., MacDonald, P. A., & Owen, A. M. (2015). Anesthesia and neuroimaging: Investigating the neural correlates of unconsciousness. *Trends in Cognitive Sciences*, *19*(2), 100–107. https://doi.org/10.1016/j.tics.2014.12.005

Magoun, H. W. (1952). An ascending reticular activating system in the brain stem. *A.M.A. Archives of Neurology and Psychiatry*, *67*(2), 145–154. https://doi.org/10.1001/archneurpsyc.1952.02320140013002

Marzano, C., Ferrara, M., Moroni, F., & De Gennaro, L. (2011). Electroencephalographic sleep inertia of the awakening brain. *Neuroscience*, *176*, 308–317. https://doi.org/10.1016/j.neuroscience.2010.12.014

Poudel, G. R., Innes, C. R., & Jones, R. D. (2013). Distinct neural correlates of time-on-task and transient errors during a visuomotor tracking task after sleep restriction. *Neuroimage*, *77*, 105–113. https://doi.org/10.1016/j.neuroimage.2013.03.054

Poudel, G. R., Innes, C. R. H., & Jones, R. D. (2018). Temporal evolution of neural activity and connectivity during microsleeps when rested and following sleep restriction. *Neuroimage*, *174*, 263–273. https://doi.org/10.1016/j.neuroimage.2018.03.031

Samann, P. G., Wehrle, R., Hoehn, D., Spoormaker, V. I., Peters, H., Tully, C., … Czisch, M. (2011). Development of the brain's default mode network from wakefulness to slow wave sleep. *Cerebral Cortex*, *21*(9), 2082–2093. https://doi.org/10.1093/cercor/bhq295

Schneider, M., Hathway, P., Leuchs, L., Samann, P. G., Czisch, M., & Spoormaker, V. I. (2016). Spontaneous pupil dilations during the resting state are associated with activation of the salience network. *Neuroimage*, *139*, 189–201. https://doi.org/10.1016/j.neuroimage.2016.06.011

Shaw, T. H., Warm, J. S., Finomore, V., Tripp, L., Matthews, G., Weiler, E., & Parasuraman, R. (2009). Effects of sensory modality on cerebral blood flow velocity during vigilance. *Neuroscience Letters*, *461*(3), 207–211. https://doi.org/10.1016/j.neulet.2009.06.008

Song, X., Qian, S., Liu, K., Zhou, S., Zhu, H., Zou, Q., … Gao, J. H. (2017). Resting-state BOLD oscillation frequency predicts vigilance task performance at both normal and high environmental temperatures. *Brain Structure & Function*, *222*(9), 4065–4077. https://doi.org/10.1007/s00429-017-1449-4

Splaingard, M., Hayes, J., & Smith, G. A. (2007). Impairment of reaction time among children awakened during stage 4 sleep. *Sleep*, *30*(1), 104–108.

Spreng, R. N., Sepulcre, J., Turner, G. R., Stevens, W. D., & Schacter, D. L. (2013). Intrinsic architecture underlying the relations among the default, dorsal attention, and frontoparietal control networks of the human brain. *Journal of Cognitive Neuroscience*, *25*(1), 74–86. https://doi.org/10.1162/jocn_a_00281

Tagliazucchi, E., & van Someren, E. J. W. (2017). The large-scale functional connectivity correlates of consciousness and arousal during the healthy and pathological human sleep cycle. *NeuroImage*, *160*, 55–72. https://doi.org/10.1016/j.neuroimage.2017.06.026

Tassi, P., & Muzet, A. (2000). Sleep inertia. *Sleep Medicine Reviews*, *4*(4), 341–353. https://doi.org/10.1053/smrv.2000.0098

Tononi, G., Massimini, M., & Riedner, B. A. (2006). Sleepy dialogues between cortex and hippocampus: Who talks to whom? *Neuron*, *52*(5), 748–749. https://doi.org/10.1016/j.neuron.2006.11.014

Trotti, L. M. (2017). Waking up is the hardest thing I do all day: Sleep inertia and sleep drunkenness. *Sleep Medicine Reviews*, *35*, 76–84. https://doi.org/10.1016/j.smrv.2016.08.005

Tsai, P. J., Chen, S. C., Hsu, C. Y., Wu, C. W., Wu, Y. C., Hung, C. S., … Lin, C. P. (2014). Local awakening: Regional reorganizations of brain oscillations after sleep. *NeuroImage*, *102*(Pt 2), 894–903. https://doi.org/10.1016/j.neuroimage.2014.07.032

Tzourio-Mazoyer, N., Landeau, B., Papathanassiou, D., Crivello, F., Etard, O., Delcroix, N., … Joliot, M. (2002). Automated anatomical labeling of activations in SPM using a macroscopic anatomical parcellation of the MNI MRI single-subject brain. *NeuroImage*, *15*(1), 273–289. https://doi.org/10.1006/nimg.2001.0978

Vallat, R., Meunier, D., Nicolas, A., & Ruby, P. (2019). Hard to wake up? The cerebral correlates of sleep inertia assessed using combined behavioral, EEG and fMRI measures. *NeuroImage*, *184*, 266–278. https://doi.org/10.1016/j.neuroimage.2018.09.033

Wong, C. W., Deyoung, P. N., & Liu, T. T. (2016). Differences in the resting-state fMRI global signal amplitude between the eyes open and eyes closed states are related to changes in EEG vigilance. *Neuroimage*, *124*, 24–31. https://doi.org/10.1016/j.neuroimage.2015.08.053

Wong, C. W., Olafsson, V., Tal, O., & Liu, T. T. (2013). The amplitude of the resting-state fMRI global signal is related to EEG vigilance measures. *Neuroimage*, *83*, 983–990. https://doi.org/10.1016/j.neuroimage.2013.07.057

Xin, F., & Lei, X. (2015). Competition between frontoparietal control and default networks supports social working memory and empathy. *Social Cognitive and Affective Neuroscience*, *10*(8), 1144–1152. https://doi.org/10.1093/scan/nsu160

Zang, Y. F., He, Y., Zhu, C. Z., Cao, Q. J., Sui, M. Q., Liang, M., … Wang, Y. F. (2007). Altered baseline brain activity in children with ADHD revealed by resting-state functional MRI. *Brain Dev*, *29*(2), 83–91. https://doi.org/10.1016/j.braindev.2006.07.002

How to cite this article: Chen X, Hsu C-F, Xu D, Yu J, Lei X. Loss of frontal regulator of vigilance during sleep inertia: A simultaneous EEG-fMRI study. *Hum Brain Mapp*. 2020;41:4288–4298. https://doi.org/10.1002/hbm.25125